Algorithm xxx: The Matlab Postprocessing Toolkit[1]

Scott A. Sarra
Marshall University
Huntington, WV

1. INTRODUCTION

Spectral methods approximate functions by projection onto a space $\mathbb{P}_N$ of orthogonal polynomials of degree $\leq N$. When the underlying function is periodic trigonometric (Fourier) polynomials are employed while a popular choice for non-periodic functions are the Chebyshev polynomials. Legendre polynomials are another option in the non-periodic case but are not as popular in applications due to the lack of a fast transform method. However spectral methods based on other, non-classical orthogonal polynomials are possible as well. For example see references [Chen et al. 2005] and [Weideman 1999]. Spectral methods yield extremely accurate approximations of smooth functions. Due to their excellent approximation properties, spectral methods have become popular in applications such as numerical partial differential equations. However, when functions are only piecewise smooth the well-known Gibbs phenomenon appears as an accuracy reduction to first order away from discontinuities and $\mathcal{O}(1)$ oscillations in the neighborhoods of jumps. The Gibbs phenomenon is illustrated in figure 1 for both the Fourier and Chebyshev approximation of the function

$$f(x) = \chi_{[-0.5,0.5]} * \sin[\cos(x)] \tag{1}$$

that will be used throughout to demonstrate the software.

A number of methods have been suggested for the purpose of reducing or eliminating the Gibbs phenomenon. They include: spectral filtering [Vandeven 1991], physical space filtering using mollifiers [Gottlieb and Tadmor 1985; Tadmor and Tanner 2002; 2005; Tadmor 2007; Tanner 2006], digital total variation filtering [Sarra 2006a], rational reconstruction [Min et al. 2007; Hesthaven et al. 2006], and a variety of direct [Gottlieb and Shu 1997; Gelb and Tanner 2006] and indirect [Shizgal and Jung 2003; Jung and Shizgal 2004] reprojection methods. The most powerful methods need to know the exact location of all discontinuities.

The purpose of this paper is to describe a Matlab software package, the Matlab Postprocessing Toolkit (MPT), that implements edge detection and postprocessing algorithms for Chebyshev and Fourier spectral methods in one and two space di-

Author's address: Scott A. Sarra, Department of Mathematics, Marshall University, 1 John Marshall Drive, Huntington, WV 25755-2560. email address: sarra@marshall.edu

mensions. The software is intended for applications, algorithm benchmarking, and educational purposes. The MPT is a significant extension and translation of the Spectral Signal Processing Suite (SSPS) [Sarra 2003c]. The SSPS was implemented in the Java programming language which limited its usefulness. The SSPS only implemented edge detection, spectral filtering, and Gegenbauer Reprojection, for one dimensional Chebyshev approximations. The MPT is implemented in a language known by a large number of scientists and engineers and is broader in the scope of algorithms implemented. Details of the available user callable M-files along with a selection of example problems and associated results may be found in the user manual distributed with the software.

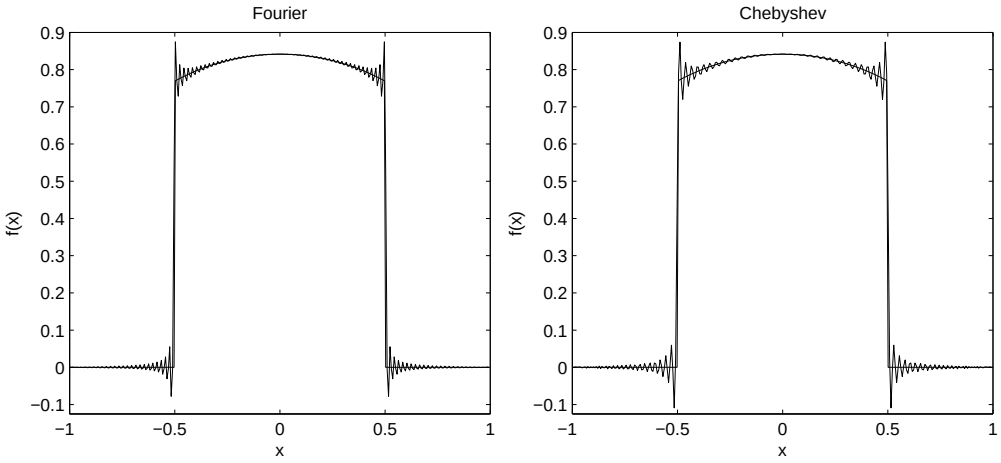

Fig. 1. Spectral approximation of function (1) vs. the exact function. The function is known at $N = 200$ interpolation sites and the interpolant is evaluated at $M = 298$ evenly spaced points. Left: Fourier. Right: Chebyshev.

2. GLOBAL POLYNOMIAL APPROXIMATION METHODS

The software package is based on interpolation, rather than expansion, methods incorporating Chebyshev and trigonometric polynomials. Interpolation and expansion methods have the same excellent approximation properties but we have chosen interpolation since pseudospectral methods for PDEs are based on interpolation. The interpolating approximation

$$\mathcal{I}_N f(x) = \sum_k a_k \, \phi_k(x) \tag{2}$$

with expansion coefficients a_k and basis functions $\phi_k(x)$ on interval $\Omega = [-1, 1]$, satisfies $\mathcal{I}_N f(x_i) = f(x_i)$ at $N + 1$ interpolation sites x_i. *Interpolation* means that $f(x)$, the function that is approximated, is a known function (at least at the interpolation sites) while the terms *collocation* and *pseudospectral* are applied to global polynomial interpolatory methods for solving differential equations for an unknown function $f(x)$. We refer to both situations as spectral approximation or

spectral methods. Detailed information on spectral methods may be found in the standard references [Boyd 2000; Canuto et al. 2006; Hesthaven et al. 2007; Reyret 2002; Trefethen 2000].

2.1 Chebyshev Interpolation

In (2) the index k runs over $k = 0, 1, \ldots, N$ and the basis functions are the Chebyshev polynomials [Mason and Handscomb 2003]

$$\phi_k(x) = T_k(x) = \cos(k \arccos(x)). \tag{3}$$

The expansion coefficients are efficiently calculated via the FFT (chebyshevCoefficients.m). The interpolation sites are the Chebyshev-Gauss-Lobatto (CGL) points

$$x_k = -\cos\left(\frac{k\pi}{N}\right) \quad k = 0, 1, \ldots, N. \tag{4}$$

The CGL points are the locations of the $N-1$ extrema of $T_N(x)$ plus the endpoints of the interval $[-1, 1]$.

2.2 Fourier (Trigonometric) Interpolation

The degree $2N$ Fourier approximation method uses evenly spaced interpolation sites

$$x_k = -1 + \frac{2}{N}k, \quad k = 0, 1, \ldots, N-1 \tag{5}$$

on $[-1, 1]$. In (2) the index k runs over $k = -N, -N+1, \ldots, N$ and the basis functions are the trigonometric polynomials

$$\phi_k(x) = e^{ik\pi x}. \tag{6}$$

The expansion coefficients are efficiently calculated via the FFT.

3. EDGE DETECTION

The majority of postprocessing algorithms either require or may incorporate the exact location of discontinuities, or edges, in the function. Edge detection methods have been developed in references [Gelb and Tadmor 1999; 2000a]. Two choices of concentration factors are available in the edge detection routines, a linear concentration factor of $\sigma(\xi) = \xi$ and an exponential concentration factor $\sigma(\xi) = \xi \exp(\frac{1}{6\xi(\xi-1)})$. Details on concentration factors can be found in references [Gelb and Tadmor 1999] and [Gelb and Tadmor 2000a].

The edges are located by examining a weighted derivative of the spectral interpolant

$$ue(x) = w\frac{d}{dx}\mathcal{I}_N f(x) \tag{7}$$

where the weight is $w = 1/N$ in the Fourier case and $w = \pi\sqrt{1-x^2}/N$ for the Chebyshev case. Denoting the location of discontinuities as α_j and defining jumps as

$$[f](x) := f(x^+) - f(x^-)$$

the convergence of $ue(x)$ to the location of the discontinuities may be described as

$$ue(x) \rightarrow \begin{cases} \mathcal{O}\left(\frac{1}{N}\right) & \text{when } x \neq \alpha_j \\ [f](\alpha_j) & \text{when } x = \alpha_j. \end{cases}$$

While a graphical examination of $ue(x)$ verifies that it does have the desired convergence properties, an additional step is needed to numerically pinpoint the location of the discontinuities. For that purpose, a non-linear enhancement [Gelb and Tadmor 2000a] is made to $ue(x)$ as

$$un(x) = N^{\frac{Q}{2}}[ue(x)]^Q.$$

The enhanced sum has the convergence properties

$$un(x) \rightarrow \begin{cases} \mathcal{O}\left(N^{\frac{-Q}{2}}\right) & \text{when } x \neq \alpha_j \\ N^{\frac{Q}{2}}\left[[f](\alpha_j)\right]^Q & \text{when } x = \alpha_j. \end{cases}$$

By choosing $Q > 1$, the separation is enhanced between the $O([\frac{1}{N}]^{\frac{Q}{2}})$ points of smoothness and the $O(N^{\frac{Q}{2}})$ points of discontinuity. The problem dependent threshold parameter J is then used to pinpoint the location of all jumps and the edges are located by redefining $ue(x)$ as

$$ue(x) = \begin{cases} ue(x) & \text{if } |un(x)| > J \\ 0 & \text{otherwise.} \end{cases}$$

Computational experience [Sarra 2003c] has lead to the inclusion of an additional parameter η which controls the number of edges that can be found in the neighborhood of a local maximum of $ue(x)$. If the maximum occurs at $x(i)$, then the parameter allows only one edge to be found in the interval $(x[i-\eta], x[i+\eta])$, $i = 0, ..., N$.

The edge detection procedure can be employed repeatedly to find discontinuities in the ℓ^{th} derivative of a function and to determine intervals of C^ℓ-smoothness. For example, to find the discontinuities in the first derivative, first the locations of the discontinuities in the function are found. Then in each smooth subinterval, $\mathcal{I}_N f(x)$ is differentiated and the edge detection procedure is applied to find the jumps in the first derivative. An example describing edge detection in a function and its first derivative can be found in reference [Gelb and Tadmor 2000b].

4. POSTPROCESSING METHODS

4.1 Spectral Filters

Spectral filters [Vandeven 1991] lessen the effects of the Gibbs phenomenon by working in transform space as

$$\mathcal{F}_N f(x) = \sum_k \sigma(k/N)\, a_k\, \phi_k(x) \tag{8}$$

The convergence rate of the filtered approximation is determined solely by the order, $\rho > 1$, of the filter and the regularity of the function away from the point of discontinuity. If the filter order, ρ, is chosen increasing with N, the filtered

expansion recovers exponential accuracy away from a discontinuity. Assuming that $f(x)$ has a discontinuity at x_0 and setting $d(x) = x - x_0$, the estimate

$$|f(x) - \mathcal{F}_N(x)| \leq \frac{K}{d(x)^{\rho-1} N^{\rho-1}} \tag{9}$$

holds where K is a constant. If ρ is sufficiently large, and $d(x)$ is not too small, the error goes to zero faster than any finite power of N, i.e. spectral accuracy is recovered. When x is close to a discontinuity the error increases. If $d(x) = \mathcal{O}(1/N)$ then the error estimate is $\mathcal{O}(1)$.

The following ρ^{th} order spectral filters are implemented in the MPT:

(1) exponential filter

$$\sigma_1(\omega) = e^{(\ln \varepsilon_m)\,\omega^\rho}, \tag{10}$$

where ρ even and ε_m represents machine zero.

(2) Erfc-Log filter [Boyd 1996]

$$\sigma_2(\omega) = \frac{1}{2}\,\mathrm{erfc}\left(2\sqrt{\rho}\,[|\omega| - 1/2]\sqrt{\frac{-\ln\left(1 - 4\,[|\omega| - 1/2]^2\right)}{4\,[|\omega| - 1/2]^2}}\right) \tag{11}$$

(3) Vandeven filter [Vandeven 1991]

$$\sigma_3(\omega) = 1 - \frac{(2\rho-1)!}{(p-1)!}\int_0^{|\omega|} t^{\rho-1}(1-t)^{\rho-1}dt. \tag{12}$$

4.2 Digital Total Variation Filtering

The Rudin, Osher, and Fatemi (ROF) Total Variation (TV) denoising model is a popular image processing method to remove noise from a digital image. The model formulates a minimization problem which leads to a nonlinear Euler-Lagrange PDE to be solved by numerical PDE methods. In [Chan et al. 2001; Osher and Shen 2000] the authors develop a discrete version of the TV model on a graph - Digital Total Variation (DTV) filtering. Viewing an oscillatory function as an image with noise, the DTV method was used to postprocess spectral approximations in [Sarra 2006a] and Radial Basis Function approximations in [Sarra 2006b]. The method works with point values in physical space and not with the spectral expansion coefficients. The DTV method does not need to know the location of edges. The point values may be located at scattered, non-structured sites, in complex geometries. The DTV method is very computationally efficient. While the method does mitigate the effects of the Gibbs phenomenon it does not make any claims of restoring spectral accuracy.

To summarize the method, let $[\Omega, G]$ be a finite set Ω of nodes and a dictionary of edges G connecting the nodes. General vertices are denoted by $\alpha, \beta, \cdots$. The notation $\alpha \sim \beta$ indicates that α and β are linked by an edge. All the neighbors of α are denoted by

$$N_\alpha = \{\beta \in \Omega \,|\, \beta \sim \alpha\}. \tag{13}$$

The graph variational problem is to minimize the fitted TV energy

$$E_\lambda^{TV}(u) = \sum_{\alpha\in\Omega} |\nabla_\alpha u|_a + \frac{\lambda}{2}\sum_{\alpha\in\Omega}(u_\alpha - u_\alpha^0)^2 \tag{14}$$

where u^0 is the spectral approximation containing the Gibbs oscillations and λ the user specified fitting parameter. The unique solution to this problem is the solution of the nonlinear restoration equation

$$\sum_{\beta\sim\alpha}(u_\alpha - u_\beta)\left(\frac{1}{|\nabla_\alpha u|_a} + \frac{1}{|\nabla_\beta u|_a}\right) + \lambda(u_\alpha - u^0_\alpha) = 0 \tag{15}$$

where the regularized location variation or strength function at any node α is defined as

$$|\nabla_\alpha u|_a = \left[\sum_{\beta\in N_\alpha}(u_\beta - u_\alpha)^2 + a^2\right]^{1/2}. \tag{16}$$

The regularization parameter a is a small (the default in the software is $a = 0.0001$) value used to prevent a zero local variation and division by zero.

The nonlinear system can be solved by a linearized Jacobi iteration as was done in [Chan et al. 2001; Sarra 2006a; 2006b]. Alternatively, we can work with the nonlinear restoration equation (15) and use time marching to reach a steady state

$$\frac{du_\alpha}{dt} = \sum_{\beta\sim\alpha}(u_\alpha - u_\beta)\left(\frac{1}{|\nabla_\alpha u|_a} + \frac{1}{|\nabla_\beta u|_a}\right) + \lambda(u_\alpha - u^0_\alpha). \tag{17}$$

Preconditioning equation (17)

$$\frac{du_\alpha}{dt} = \sum_{\beta\sim\alpha}(u_\alpha - u_\beta)\left(1 + \frac{|\nabla_\alpha u|_a}{|\nabla_\beta u|_a}\right) + \lambda\,|\nabla_\alpha u|_a\,(u_\alpha - u^0_\alpha). \tag{18}$$

yields a faster convergence to the steady state [Osher and Shen 2000]. The software uses time marching with the explicit Euler's method. Typically about 100 time steps are required to approach a steady state. An optimal value of the fitting parameter λ is not known. However, a large range of values for the fitting parameter results in a "good" postprocessing. In general, stronger oscillations are best handled with a small fitting parameter (< 10) while weaker oscillations require a larger value of the fitting parameter. More details on selecting the value of the shape parameter can be found in references [Sarra 2006a] and [Sarra 2009].

In two space dimensions there is more than one way to define N_α (figure 2). One is to consider at a node $\alpha_{i,j}$ four neighboring points,

$$N^4_\alpha = \{\alpha_{i,j+1}, \alpha_{i+1,j}, \alpha_{i,j-1}, \alpha_{i-1,j}\}$$

and another is an eight point neighborhood,

$$N^8_\alpha = \{\alpha_{i,j+1}, \alpha_{i+1,j+1}, \alpha_{i+1,j}, \alpha_{i+1,j-1}, \alpha_{i,j-1}, \alpha_{i-1,j-1}, \alpha_{i-1,j}, \alpha_{i-1,j+1}\}.$$

4.3 Rational Reconstruction

Rational functions have been used in several different forms to reduce the Gibbs phenomenon [Clenshaw and Lord 1974; Driscoll and Fornberg 2001; Hesthaven and Kaber 2008; Hesthaven et al. 2006; Min et al. 2007]. Rational functions are more complex than simple polynomials and often do better in approximation discontinuous functions or functions with steep gradients.

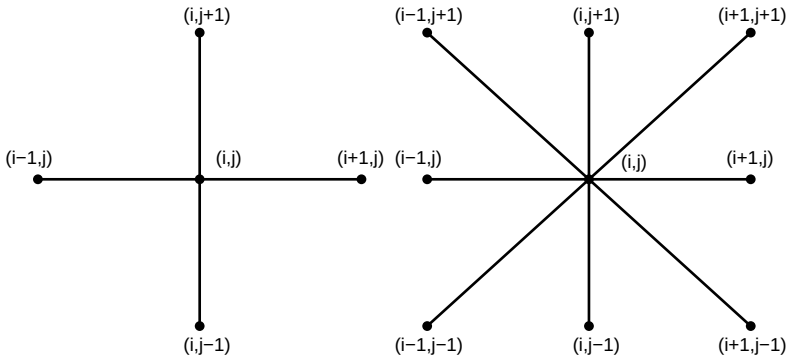

Fig. 2. 2d DTV neighborhoods: Left, N_α^4. Right: N_α^8

A Padé approximant is of the form

$$R_{K,M} = \frac{P_K}{Q_M} = \frac{\sum_{k=0}^{K} p_k \phi_k(x)}{\sum_{m=0}^{M} q_m \phi_m(x)} \tag{19}$$

The linear Padé approximation of a function u is determined by imposing the orthogonality relations

$$\langle Q_M u - P_K, \phi \rangle = 0, \qquad \forall \phi \in \mathbb{P}_N \tag{20}$$

From this, a linear system with $M+1$ unknowns and $K-N$ equations can be extracted. Reference [Hesthaven and Kaber 2008] can be consulted for details. After the degree of the denominator M is chosen the degree of the numerator is set as $K = (N - N_c) - M$ where $N_c <= N$ is a cutoff value that specifies how many of the high order expansion coefficients are not used to form the Padé approximation. This is necessary since a significant portion of the high modes are polluted when discontinuous functions are approximated [Hesthaven et al. 2006; Min et al. 2007]. This results in a linear system with one more unknown than equation. In the Chebyshev case (chebyshevPade.m based on [Clenshaw and Lord 1974]) this is resolved by setting $q_0 = 1$ which leaves a $M \times M$ linear system to be solved for $q_1, \ldots, q_M$. In the Fourier case (fourierPade.m) we have followed the method outlined in [Min et al. 2007].

The rational reconstruction code of the MPT does not incorporate edge detection. However, if we are to recover spectral accuracy at the point of a discontinuity [Driscoll and Fornberg 2001] or to accurately postprocess computational data from a PDE problem, it will be necessary to use the locations of discontinuities. A discussion of how to incorporate edge detection into the rational reconstruction algorithms and numerical examples can be found in reference [Hesthaven et al. 2006].

4.4 Reprojection Methods

Reprojection methods take the spectral projection and project in onto another basis. In the new basis, spectral accuracy is recovered. Let $\xi(x)$ be the map that takes $x \in [a, b]$ to $\xi \in [-1, 1]$ and let $x(\xi)$ be the inverse of the map. In each of the

i smooth subintervals $[a, b]$ the function is reprojected as

$$f_P^i(x) = \sum_{\ell=0}^{m_i} g_\ell^i \Psi_\ell[\xi(x)] \tag{21}$$

onto a basis $\Psi_\ell(x)$ of polynomials, the reprojection basis, which are orthogonal on $[-1, 1]$ with respect to a weight function $w(x)$ under the weighted inner product $(\Psi_k(\xi), \Psi_k(\xi))_w$ which satisfies

$$(\Psi_k(\xi), \Psi_\ell(\xi))_w = \int_{-1}^{1} \Psi_k(\xi)\Psi_\ell(\xi)w(\xi)d\xi = \gamma_\ell \delta_{k\ell} \tag{22}$$

where γ_ℓ is a normalization factor. The expansion coefficients g_ℓ^i are evaluated via a Gaussian quadrature formula. If the function being approximated is known at the quadrature points, g_ℓ^i are referred to as the exact reprojection coefficients. Otherwise the spectral interpolant (2) is used to approximate the function at the quadrature points and the coefficients are referred to as the approximate reprojection coefficients $\hat{g}_\ell^i$.

The accuracy of the reprojection methods depends on accurately locating all discontinuities and intervals of smoothness. Failure to identify a discontinuity will cause the methods to fail badly. However, the methods are fairly robust to misidentifying the location of a discontinuity within a cell or two. This is because the weight of the reprojection basis tapers smoothly to zero at its boundaries and the reprojection coefficients are computed by multiplying the original function or its spectral projection by the reprojection weight. In the neighborhood of discontinuities, the result of the multiplication is very small if the weight is properly designed and crossing a discontinuity by a few cells will only result in a correspondingly small error.

4.4.1 *Gegenbauer Reprojection.* The Gegenbauer Reprojection Procedure (GRP) uses the Gegenbauer or Ultraspherical polynomials C_ℓ^λ as the reprojection basis. The GRP was developed in the series of papers [Gottlieb et al. 1992; Gottlieb and Shu 1994; 1996; 1995a; 1995b; 1997]. Further analysis and application of the GRP can be found in references [Boyd ; Jackiewicz 2003; Sarra 2003a; 2003b]. Reference [Boyd] describes how the convergence of the GRP is adversely affected when the underlying function has singularities off the real axis.

The Gegenbauer polynomials satisfy the conditions of a Gibbs complementary basis [Hesthaven et al. 2007] which allows for a spectrally accurate reprojection. The weight function associated with the Gegenbauer polynomials is $w(x) = (1 - \xi^2)^{\lambda-1/2}$. The Gegenbauer polynomials (gegenbauerPolynomial.m) are calculated via the three term recurrence relation

$$C_{k+1}^\lambda(\xi) = \frac{2(k+\lambda)\xi}{k+1} C_k^\lambda(\xi) - \frac{k+2\lambda-1}{k+1} C_{k-1}^\lambda(\xi), \qquad k = 1, 2, \ldots \tag{23}$$

with $C_0^\lambda = 1$ and $C_1^\lambda = 2\lambda\xi$.

In smooth subinterval i the GRP postprocessed approximation is

$$f_P^i(x) = \sum_{\ell=0}^{m_i} g_\ell^i C_\ell^\lambda[\xi(x)] \tag{24}$$

where the exact Gegenbauer expansion coefficients are

$$g_\ell^i = \frac{1}{\gamma_\ell^\lambda}\int_{-1}^{1}(1-\xi^2)^{\lambda-1/2}C_\ell^\lambda(\xi)f[x(\xi)]d\xi \tag{25}$$

and

$$\gamma_\ell^\lambda = \pi^{\frac{1}{2}}\frac{\Gamma(\ell+2\lambda)\Gamma(\lambda+\frac{1}{2})}{\ell!\Gamma(2\lambda)\Gamma(\lambda)(n+\lambda)}.$$

If only the expansion coefficients a_k are known and not the underlying function, as in a pseudospectral PDE approximation, the Gegenbauer coefficients are replaced with the approximate Gegenbauer coefficients

$$\hat{g}_\ell^i = \frac{1}{\gamma_\ell^\lambda}\int_{-1}^{1}(1-\xi^2)^{\lambda-1/2}C_\ell^\lambda(\xi)\mathcal{I}_N f[x(\xi)]d\xi. \tag{26}$$

The integrals in (25) and (26) are evaluated via Chebyshev-Gauss-Lobatto quadrature.

4.4.2 *Freud Reprojection.* The Freud Reprojection Procedure (FRP) [Gelb 2007; Gelb and Tanner 2006] uses the Freud polynomials ψ as the reprojection basis and the weight function is $w(\xi) = e^{-c\xi^{2\lambda}}$ where $\lambda = \alpha N$, $0 < \alpha < 1$, and $c = \ln\epsilon_M$ where ϵ_M is machine epsilon. We have used $\lambda = \text{round}\left(\sqrt{N(b-a)/2} - 2\sqrt{(2)}\right)$ which was suggested in [Gelb and Tanner 2006].

In [Gelb and Tanner 2006] an additional condition is added to the three conditions that a Gibbs complementary basis must satisfy. A basis that satisfies the four conditions is called a Robust Gibbs complement. The Freud polynomial basis is an example of a Robust Gibbs complement. Freud reprojection does not suffer from the numerical roundoff errors and the Runge phenomenon that the GRP does [Boyd]. The Freud polynomials are not known explicitly but can be computed recursively as

$$\psi_{k+1}(\xi) = \xi\psi_k(\xi) - \frac{\gamma_k}{\gamma_{k-1}}\psi_{k-1}(\xi)$$

where $\psi_0(\xi) = 1$ and $\psi_1(\xi) = \xi$. The recursion coefficients are

$$\gamma_k = (\psi_k(\xi), \psi_k(\xi))_w = \int_{-1}^{1}\psi_k(\xi)\psi_k(\xi)e^{-c\xi^{2\lambda}}d\xi. \tag{27}$$

The exact Freud coefficients are

$$g_\ell^i = \frac{1}{\gamma_\ell}\int_{1}^{-1}e^{-c\xi^{2\lambda}}\psi_\ell(\xi)f[x(\xi)]d\xi. \tag{28}$$

and the approximate Freud coefficients are

$$\hat{g}_\ell^i = \frac{1}{\gamma_\ell}\int_{1}^{-1}e^{-c\xi^{2\lambda}}\psi_\ell(\xi)\mathcal{I}_N f[x(\xi)]d\xi. \tag{29}$$

Integrals (27), (28), and (29) are evaluated very accurately using the trapezoid rule which is exponentially accurate for smooth periodic functions. In smooth

subinterval i the FRP approximation is

$$f_P^i(x) = \sum_{\ell=0}^{m_i} g_\ell^i \psi_\ell[\xi(x)]. \tag{30}$$

In each subinterval of smoothness m_i is set $m_i = N(b-a)/8$. However, as N increases the number of terms in the reprojection basis m_i is more than is necessary to numerically resolve the function and the higher numbered reprojection coefficients become very close to machine epsilon which leads to round-off errors. As described on p. 15 of [Gelb and Tanner 2006], the round-off errors can be avoided by resetting m_i to a value that prevents the average of three consecutive reprojection coefficients from being larger than a specified tolerance. Experimentally we have found a tolerance of 10e-12 to work well in the Fourier case and 10e-8 to work well with Chebyshev approximations.

For the FRP, the specification of M is not function-dependent as is the case for the GRP. The FRP does not have any function-dependent parameters to be supplied by the user. This is in contrast to the GRP which depends heavily on the proper specification of both a weight parameter λ and reprojection order M. Numerical evidence indicates that the FRP recovers exponential accuracy. However, due to the incomplete knowledge of the Freud polynomials, this result has not been proven to hold.

4.4.3 *Inverse Reprojection.* The Gegenbauer and Freud reprojection methods are referred to as direct methods as they compute the reprojection coefficients directly from the spectral expansion coefficients a_k (or function values). In contrast, inverse methods compute the reprojection coefficients by solving a linear system of equations

$$Wg = a.$$

The Inverse Reprojection method was developed in [Jung and Shizgal 2004; 2005; Shizgal and Jung 2003]. A recent application of the Inverse Reprojection method to time-dependent PDE solutions can be found in [Abdi and Hosseini 2008]. Originally [Shizgal and Jung 2003], the Gegenbauer polynomials were used as the reprojection basis, but later [Jung and Shizgal 2004; 2005] the method was generalized to yield a unique reconstruction using any set of basis functions. The generalized method is referred to as the inverse polynomial reconstruction method (IPRM).

We have implemented the method using the Gegenbauer polynomials as the reconstruction basis. Note that since the IPRM uniquely determines the reconstruction for any reconstruction basis, the Gegenbauer parameter λ does not play a role in the method as it does in the GRP method. The matrix W may be very ill-conditioned. This problem is addressed in reference [Jung and Shizgal 2007]. The conditioning of W is best for small $\lambda > 0$ [Shizgal and Jung 2003]. In the computer code the default is $\lambda = 1/2$ which corresponds to the Legendre basis. Care has been taken to consistently evaluate the spectral expansion coefficients and the integrals that determine the elements of the matrix W as is discussed in [Jung and Shizgal 2004]. Both are evaluated using Gaussian quadrature.

5. GRAPHICAL USER INTERFACE

The Matlab functions of the MPT may be called directly from user written Matlab code as we have illustrated in the examples provided in the user manual that accompanies the software. Additionally, to make the MPT functions more accessible to non-Matlab users a graphical user interface (GUI) has been developed. The GUI has built-in functions and pseudospectral PDE solutions that can be used to demonstrate and benchmark the algorithms. The Fourier PDE examples include linear advection and inviscid Burger's equation and the Chebyshev examples include linear advection and the Euler equations of gas dynamics. More details of the GUI may be found in the GUI user guide which is also include with the distributed software. A screen shot of the GUI is shown in figure 3.

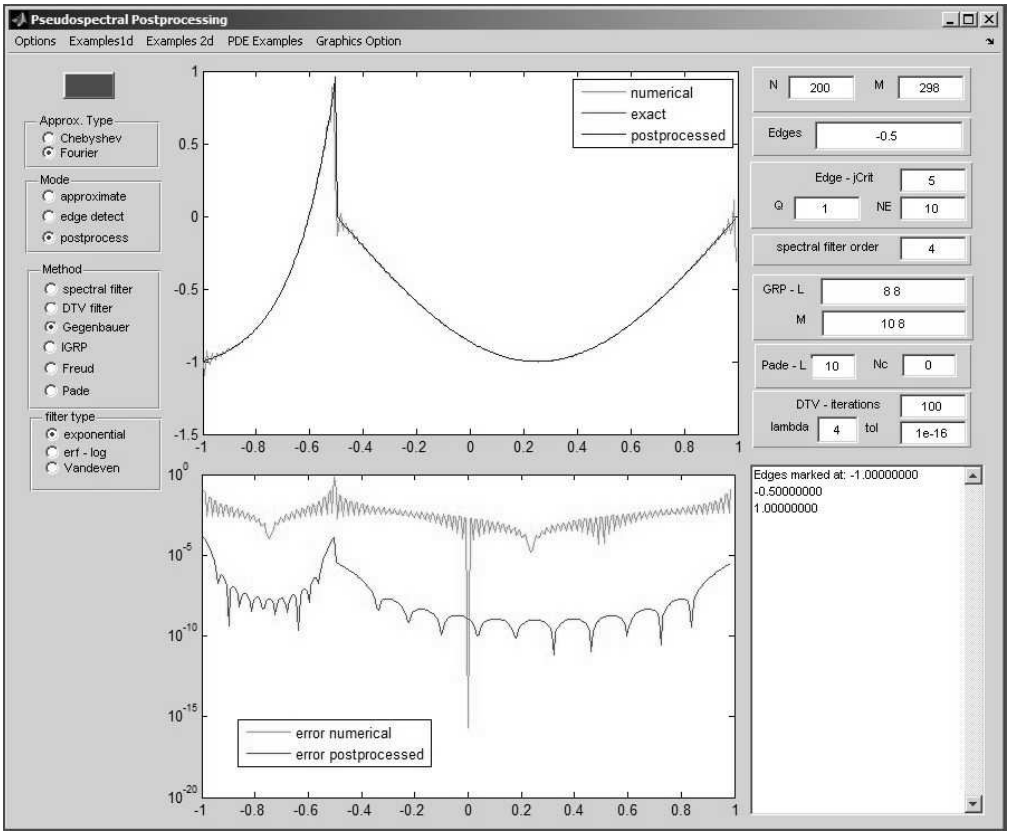

Fig. 3. Graphical user interface

6. CONCLUDING COMMENTS

We have described a suite of Matlab programs that implement state-of-the-art postprocessing and edge detection algorithms for Fourier and Chebyshev spectral approximations of piecewise smooth functions in one and two space dimensions.

Postprocessing methods that require one or more user defined parameters be specified in each smooth subregion are difficult to implement in two space dimensions. For this reason, the MPT only implements spectral filtering and DTV filtering in two dimensions. Although not the most powerful one dimensional methods, they are very computationally efficient and the closest to "black box" algorithms in two dimensions. In two dimensional applications, many of the one dimensional methods can been applied to one dimensional slices in the x or y direction. This approach has been taken in references [Jung and Shizgal 2005] and [Min et al. 2007].

The MPT functions may be called directly from a Matlab script. Alternatively, the routines may be accessed from a GUI. The postprocessing functions and accompanying GUI with built-in example functions and PDE solutions provide users the opportunity to benchmarch and demonstrate the postprocessing algorithms. Experienced Matlab users will find it easy to modify the GUI to incorporate their own algorithms or example problems. The development of the MPT is ongoing and modifications and extensions will be made as new algorithms are developed.

We conclude with table 6 that summarizes the basic feature of the postprocessing algorithms.

method	edge detection	parameters	spectral accuracy	large $\kappa(A)$
spectral filter		ρ	$\sim$	
DTV		λ		
Padé	$\sim$	M, N_c		$\surd$
GRP	$\surd$	λ, m_i	$\surd$	
FRP	$\surd$		$\surd^*$	
IPRM	$\surd$	m_i	$\surd$	$\surd$

A $\surd$ in the edge detection column indicates the method must know the exact location of the discontinuities while a $\sim$ indicates that the edge location may be incorporated to improve the method. The parameters column lists any user specified parameters. If the method incorporates edge detection the parameters must be specified in each subinterval of smoothness. A $\surd$ in the spectral accuracy column indicates the method is able to recover spectral accuracy over the entire interval while a $\sim$ indicates that spectral accuracy may be recovered over a portion of the interval sufficiently away from the edge locations. The $\surd^*$ in the spectral accuracy column of the FRP indicates numerically observed but not theoretical proven spectral accuracy. A $\surd$ in the large $\kappa(A)$ column indicates that a linear system must be solved to implement the method and that the matrix may have a large condition number.

REFERENCES

Abdi, A. and Hosseini, S. M. 2008. An investigation of resolution of 2-variate Gibbs phenomenon. *Applied Mathematics and Computation 203*, 714–732.

Boyd, J. P. Trouble with Gegenbauer reconstruction for defeating Gibbs' phenomenon: Runge phenomenon in the diagonal limit of Gegenbauer polynomial approximations. *Journal of Computational Physics*.

Boyd, J. P. 1996. The Erfc-Log filter and the asymptotics of the Vandeven and Euler sequence accelerations. *Houston Journal of Mathematics*, 267–275.

Boyd, J. P. 2000. *Chebyshev and Fourier Spectral Methods*, second ed. Dover.

Canuto, C., Hussaini, M., Quarteroni, A., and Zang, T. 2006. *Spectral Methods: Fundamentals in Single Domains*. Springer.

Chan, T., Osher, S., and Shen, J. 2001. The digital TV filter and nonlinear denoising. *IEEE Transactions on Image Processing 10,* 2.

Chen, Q., Gottlieb, D., and Hesthaven, J. 2005. Spectral methods based on prolate spheroidal wave functions for hyperbolic PDEs. *SIAM Journal on Numerical Analysis 43,* 5, 1912–1933.

Clenshaw, C. W. and Lord, K. 1974. Rational approximations from Chebyshev series. In *Studies in Numerical Analysis*, B. Scaife, Ed. Academic Press, 95113.

Driscoll, T. and Fornberg, B. 2001. A Padé-based algorithm for overcoming the Gibbs phenomenon. *Numerical Algorithms 26*, 77–92.

Gelb, A. 2007. Reconstruction of piecewise smooth functions from non-uniform grid data. *Journal os Scientific Computing 30,* 3, 409–440.

Gelb, A. and Tadmor, E. 1999. Detection of edges in spectral data. *Applied and Computational Harmonic Analysis 7*, 101–135.

Gelb, A. and Tadmor, E. 2000a. Detection of edges in spectral data II: Nonlinear enhancement. *SIAM Journal of Numerical Analysis 38,* 4, 1389–1408.

Gelb, A. and Tadmor, E. 2000b. Enhanced spectral viscosity approximations for conservation laws. *Applied Numerical Mathematics 33*, 3–21.

Gelb, A. and Tanner, J. 2006. Robust reprojection methods for the resolution of the Gibbs phenomenon. *Applied and Computational Harmonic Analysis 20*, 3–25.

Gottlieb, D. and Shu, C.-W. 1994. Resolution properties of the Fourier method for discontinuous waves. *Comput. Methods Appl. Mech. Engrg. 116*, 27–37.

Gottlieb, D. and Shu, C.-W. 1995a. On the Gibbs phenomenon IV: Recovering exponential accuracy in a subinterval from a Gegenbauer partial sum of a piecewise analytic function. *Mathematics of Computation 64*, 1081–1095.

Gottlieb, D. and Shu, C.-W. 1995b. On the Gibbs phenomenon V: Recovering exponential accuracy from collocation point values of a piecewise analytic function. *Numerische Mathematik 71*, 511–526.

Gottlieb, D. and Shu, C.-W. 1996. On the Gibbs phenomenon III: Recovering exponential accuracy in a subinterval from a partial sum of a piecewise analytic function. *SIAM Journal of Numerical Analysis 33*, 280–290.

Gottlieb, D. and Shu, C.-W. 1997. On the Gibbs phenomenon and its resolution. *SIAM Review 39,* 4, 644–668.

Gottlieb, D., Shu, C.-W., Solomonoff, A., and Vandeven, H. 1992. On the Gibbs phenomenon I: recovering exponential accuracy from the Fourier partial sum of a nonperiodic analytic function. *Journal of Computational and Applied Mathematics 43*, 81–98.

Gottlieb, D. and Tadmor, E. 1985. Recovering pointwise values of discontinuous data within spectral accuracy. In *Progress and Supercomputing in Computational Fluid Dynamics*, E. M. Murman and S. S. Abarbanel, Eds. Birkhäuser, Boston, 357–375.

Hesthaven, J., Gottlieb, S., and Gottlieb, D. 2007. *Spectral Methods for Time-Dependent Problems*. Cambridge University Press.

Hesthaven, J. and Kaber, S. 2008. Padé-Jacobi approximants. *Under Review. Journal of Computational and Applied Mathematics*.

Hesthaven, J., Kaber, S., and Lurati, L. 2006. Padé-Legendre interpolants for Gibbs reconstruction. *Journal of Scientific Computing 28,* 2-3, 337–359.

Jackiewicz, Z. 2003. Determination of optimal parameters for the Chebyshev-Gegenbauer reconstruction method. *SIAM Journal of Scientific Computing 25,* 4.

Jung, J.-H. and Shizgal, B. 2004. Generalization of the inverse polynomial reconstruction method in the resolution of the Gibbs phenomenon. *Journal of Computational and Applied Mathematics 172*, 131–151.

Jung, J.-H. and Shizgal, B. 2005. Inverse Polynomial Reconstruction of Two Dimensional Fourier Images. *Journal of Scientific Computing 25*, 367–399.

Jung, J.-H. and Shizgal, B. 2007. On the numerical convergence with the inverse polynomial reconstruction method for the resolution of the Gibbs phenomenon. *Journal of Computational Physics 224*, 477–488.

Mason, J. and Handscomb, D. 2003. *Chebyshev Polynomials*. CRC.

Min, M. S., Kaber, S. M., and Don, W. S. 2007. Fourier-Padé approximations and filtering for spectral simulations of an incompressible Boussinesq convection problem. *Mathematics of Computation 76*, 1275–1290.

Osher, S. and Shen, J. 2000. Digitized PDE method for data restoration. In *Analytic-Computational Methods in Applied Mathematics*, G. Anastassiou, Ed. Chapman and Hall/CRC, Chapter 16, 751–771.

Reyret, R. 2002. *Spectral Methods for Incompressible Viscous Flow*. Springer.

Sarra, S. A. 2003a. Chebyshev super spectral viscosity method for a fluidized bed model. *Journal of Computation Physics 186,* 2, 630–651.

Sarra, S. A. 2003b. Spectral methods with postprocessing for numerical hyperbolic heat transfer. *Numerical Heat Transfer 43,* 7, 717–730.

Sarra, S. A. 2003c. The spectral signal processing suite. *ACM Transactions on Mathematical Software 29,* 2.

Sarra, S. A. 2006a. Digital Total Variation filtering as postprocessing for Chebyshev pseudospectral methods for conservation laws. *Numerical Algorithms 41*, 17–33.

Sarra, S. A. 2006b. Digital Total Variation filtering as postprocessing for Radial Basis Function Approximation Methods. *Computers and Mathematics with Applications 52*, 1119–1130.

Sarra, S. A. 2009. Edge detection free postprocessing for pseudospectral approximations. *To appear in the Journal of Scientific Computing*.

Shizgal, B. and Jung, J.-H. 2003. Towards the resolution of the Gibbs phenomena. *Journal of Computational and Applied Mathematics 161*, 41–65.

Tadmor, E. 2007. Filters, mollifiers and the computation of the Gibbs phenomenon. *Acta Numerica 16*, 305–378.

Tadmor, E. and Tanner, J. 2002. Adaptive mollifers - high resolution recovery of piecewise smooth data from its spectral information. *Foundations of Computational Mathematics 2*, 155–189.

Tadmor, E. and Tanner, J. 2005. Adaptive filters for piecewise smooth spectral data. *IMA Journal of Numerical Analysis 25,* 4.

Tanner, J. 2006. Optimal filter and mollifier for piecewise smooth spectral data. *Mathematics of Computation 75,* 254.

Trefethen, L. N. 2000. *Spectral Methods in Matlab*. SIAM, Philadelphia.

Vandeven, H. 1991. Family of spectral filters for discontinuous problems. *SIAM Journal of Scientific Computing 6*, 159–192.

Weideman, J. 1999. Spectral methods based on nonclassical orthogonal polynomials. *International Series of Numerical Mathematics 31*, 239–251.